Sub-nanosecond excitonic luminescence in ZnO:In nanocrystals

Larisa Grigorjeva[a,*], Jurgis Grube[a], Ivita Bite[a], Aleksejs Zolotarjovs[a], Krisjanis Smits[a], Donats Millers[a], Piotr Rodnyi[b], Kirill Chernenko[b]

[a] Institute of Solid State Physics, University of Latvia, Latvia
[b] Peter the Great St. Petersburg Polytechnic University, St. Petersburg, Russian Federation

ARTICLE INFO

Keywords:
ZnO:In
Time-resolved luminescence
Indium doping
Scintillation

ABSTRACT

The effects of indium concentration influence on the morphology, luminescence spectra and luminescence decay kinetics of ZnO:In nanocrystals prepared by the solar physical vapour deposition method are investigated. While undoped ZnO nanocrystals exhibit tetrapod-like morphology, with increasing indium concentration the tetra-pods are transformed into particles whose average size decreases with increasing indium concentration. The results of time-resolved luminescence studies of undoped and indium doped ZnO nanocrystals showed that by increasing indium concentration the decay time falls and luminescence intensity decreases.

1. Introduction

It is well-known that ZnO has excellent luminescence characteristics - especially fast intrinsic luminescence (Kano et al., 2011; Wilkinson et al., 2004). In addition, ZnO possesses fast near band (NB) excitonic luminescence at 300K with decay times in sub-nanosecond time region. The NB luminescence band with a maximum in UV spectral range and sub-nanosecond decay time has an excitonic nature (Wilkinson et al., 2004) and can be observed even at room temperature. This effect possibly can be used for fast scintillator technology development. Along with NB luminescence, the luminescence of defect states in 450–650 nm spectral regions with decay times in microsecond region is usually present. In recent years the ZnO optical ceramics were produced by uniaxial hot pressing in a high-temperature vacuum furnace (Gorokhova et al., 2015; Rodnyi et al., 2012) and the effects of doping and scintillation properties of ZnO ceramics are intensively in-vestigated. These studies are accompanied with doped single crystal experiments that showed a dopant-induced significant decrease in the lifetime of exciton luminescence (Kano et al., 2011). Determination of the decay time of exciton luminescence at 300K requires a methodology with a high time response (pump-probe experiments) since this lumi-nescence is in picosecond time region (Wilkinson et al., 2004). For example, in ZnO, ZnO:Fe single crystals double exponential decay (1.7 ns and 0.19 ns for ZnO and 0.13 ns and 74 ps for ZnO:Fe) was observed. However, ZnO:In single crystals give only fast 15 ps luminescence decay (Kano et al., 2011); and this is the shortest decay time registered to date. ZnO:In were prepared by different methods and in different forms: as single crystals, nanofibers and thin films. Optical properties of these samples vary significantly. In addition, some studies show the ZnO:In films prepared by spray pyrolysis method exhibiting excellent electrical properties and transparency (Wienke and Booi, 2008); however, unfortunately the luminescence properties are not studied for these films.

Moreover, recently (Chernenko et al., 2018) it was found that doping with Ga or In suppresses the defect luminescence in optical ceramics made of ZnO. A similar effect was observed in ZnO:In nanowires at low doping level. Suppression of defect luminescence with microsecond decay times is very important for fast scintillators; however, sub-nanosecond luminescence in ZnO:In NC was not explored previously. In this work we present the results of time-resolved luminescence studies accompanied by the morphology studies of undoped and indium doped ZnO nanocrystals (NC) obtained via the solar physical vapour deposition (SPVD) method (Smits et al., 2014).

2. Materials and methods

The SEM, XRD and XRF were used for ZnO:In NC characterization (indium concentrations in target were 0.5; 1.0; 2.0 and 3.0 wt%). SEM measurements were performed on a microscope LYRA3 TESCAN. Indium concentration was estimated using X-ray fluorescence analyser (XRF) EDAX Eagle III XPL. X-ray diffraction spectra (XRD) for crystalline structure studies were taken using PANalytical X'Pert Pro diffractometer.

Photoluminescence was measured using wavelength-tuneable picosecond (30 ps) solid state laser with laser pulse energy around 160 μJ/cm^2. Excitation wavelength was set at 266 nm. The laser beam was focused on the sample using convex lens. Laser beam spot size was

* Corresponding author.
E-mail address: lgrig@latnet.lv (L. Grigorjeva).

Table 1
Indium concentration in target for SPVD and in resulting powder (estimated from XRF).

In2O3 in target, wt.%	Indium wt.% in powder	Indium at.% in powder	Indium mol.% in powder
0.5	0.55	0.20	0.1
1.0	0.94	0.24	0.12
2.0	1.35	0.40	0.2
3.0	3.65	1.01	0.5
0	0	0	0

around 6 mm^2. For spectral selection (dispersion) we used Bruker 250IS/SM spectrograph with grating 150 l/mm at blaze 300 nm.

The x-ray excitation was used for radioluminescence spectra measurements. Spellman XLF60N1200/230 power supply coupled to the W anode X-Ray tube with 0.1 mm Be window is used in cryostat. The lamp power is set to 30 kV; 10 mA.

In the present study ZnO:In nanopowders were obtained in a Heliotron reactor (PROMES CNRS, France) via the solar physical vapour deposition (SPVD) method (Smits et al., 2014). The method of preparation offers many advantages over the conventional methods: outstanding purity of the samples, ease of doping, ability to acquire huge temperature gradient and the process itself is ecologically-friendly.

3. Sample characterization

In Table 1 the results of XRF measurements for indium concentration estimation in ZnO:In powders prepared by SPVD method are presented. During the vapour deposition process the indium was incorporated inside the ZnO NCs. The concentration of Indium after SPVD correlates well with the concentration in target.

One of the possible mechanisms of how the indium can be implemented in ZnO matrix is In^{3+} substitution of Zn^{2+}. In this case, for the charge compensation two In atoms as well as one additional oxygen atom are necessary.

Analysis of XRD results gives only one h-ZnO phase. Additional phases or separate In_2O_3 phase were not detected. For this study is important that the concentration of indium in powder is in range of one crystalline phase ZnO:In. (Hoel et al., 2010). This suggests that the studied concentration of indium is small and In incorporates in Zn site (Fig. 1).

In Fig. 2a-d SEM images of powders with different indium concentrations are shown. One can see that the morphology and particle size heavily depend on indium concentration. The tetrapod like particles were observed in undoped ZnO nanocrystals and in samples with 0.5 wt%In. With the growth of indium concentration the morphology changes significantly.

4. Results and discussion

In undoped ZnO nanocrystals the tetrapod particles were observed which is very common for ZnO nanopowders prepared by SPVD and some others methods. The particle shape changes slightly from tetrapods to whiskers for 0.5 wt% In concentration. Such low concentration of indium does not significantly affect the formation of nanoparticles

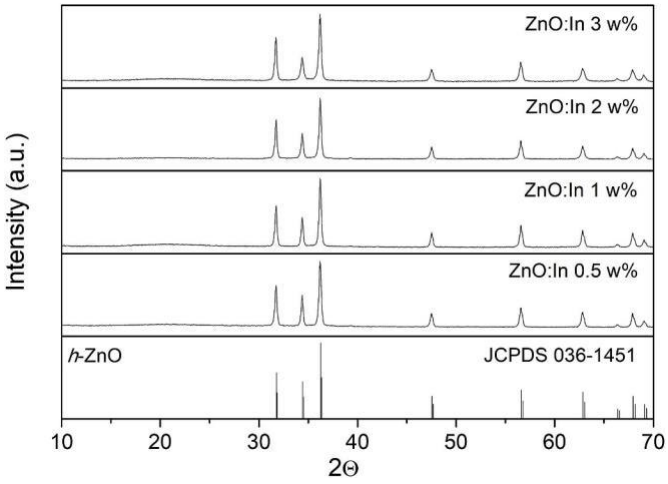

Fig. 1. XRD results of ZnO:In NCs.

(Fig. 2a) and tetrapods and nanowires are still observed; however, to a much lower extent. With increasing indium concentration, the tetra-pods are transformed into spherical particles. At concentration of 1.0 wt % nanoparticle aggregates are formed and there are particles down to 1 μm. The average size decreases with increasing indium concentration even further: a fairly uniform powder with a diameter of particles 100–200 nm was detected at concentration of 3.0 wt% In (Fig. 2d).

Near band luminescence in ZnO single crystals is studied due to specific exciton processes – free, bound excitons and their phonon replicas. Two important properties - decay time of excitonic luminescence is in sub-nanosecond time region and large exciton binding energy, allowing registering exciton luminescence at room temperature. Doping with Al, Ga, In leads to the formation of shallow donor levels and is accompanied with fast luminescence. However, the mechanisms of luminescence are not clear and are subject to studies. In the present study the indium doped nanopowders were prepared, the morphology of powders and luminescence decay time dependence on indium concentration was investigated. In Fig. 3 the temperature dependence of radioluminescence spectra in region of exciton bands in undoped and indium doped ZnO NC is shown. The well-known (Meyer et al., 2004) narrow bands are observed at low temperature in undoped samples. This is explained with exciton bound at donor ExD^0 (3.36 eV) and its phonon replicas as well as phonon replicas of free exciton LO_FEx (3.31 eV). The observed spectrum (Fig. 3, spectrum A) indicates good quality of synthesized NCs as no artefacts are present. It is observed that the low temperature spectrum of ZnO:In differs significantly from un-doped ZnO NCs.

In the low temperature radioluminescence spectra the ExD0 luminescence in ZnO:In is hidden under additional absorption occurring due to the impurities or defects associated with it. Usually this luminescence band in single crystal is at 3.36 eV at 9K. The luminescence at 3.31 eV is 1LO_FEx band; however, the band position slightly shifts with tem-perature increase and at 300K the peak position is at 3.27 eV. It is significantly broadened in comparison to the undoped sample. The 3.22 eV band coincides with DAP luminescence in single crystals (Meyer et al., 2004; Xiong et al., 2005) and wide band peaking at 2.96 eV (at 9K) is characteristic of indium doped nanopowders. How-ever, this luminescence is quenched at the temperature of ~150K and

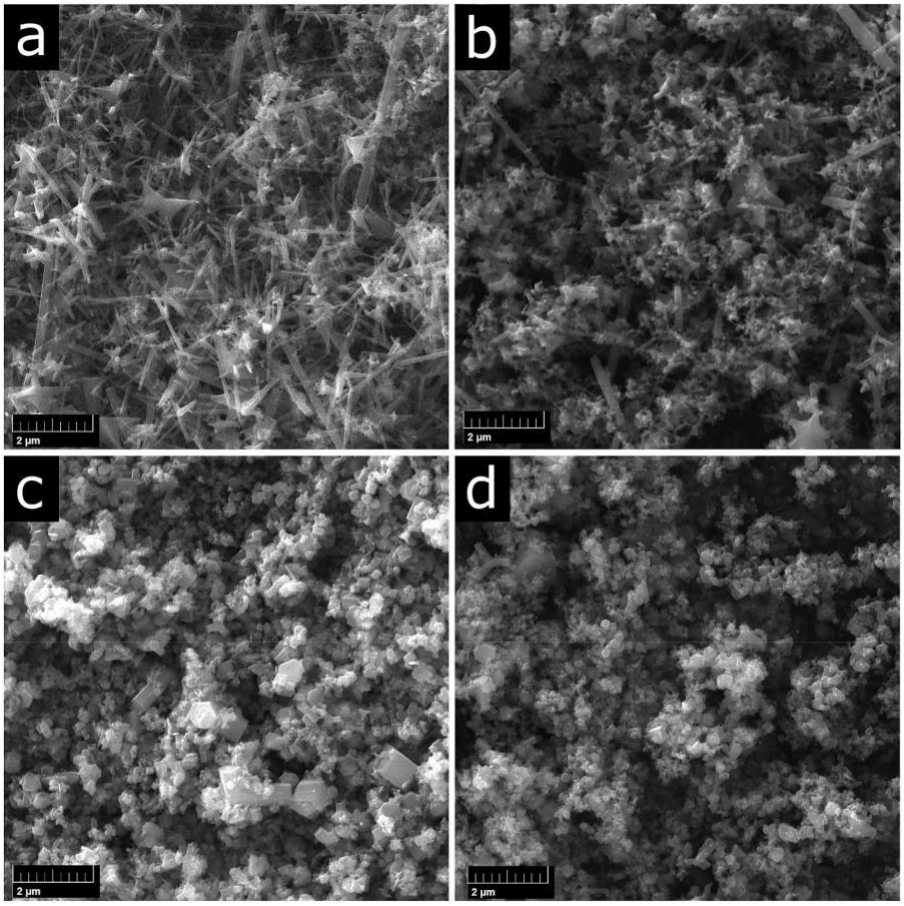

Fig. 2. SEM images of ZnO:In NC at different concentrations of In_2O_3 in targets**. a -** 0.5 wt% In_2O_3 in target, **b** - 1 wt% In_2O_3 in target, **c** - 2 wt% In_2O_3 in target, **d** - 3 wt% In_2O^3 in target.

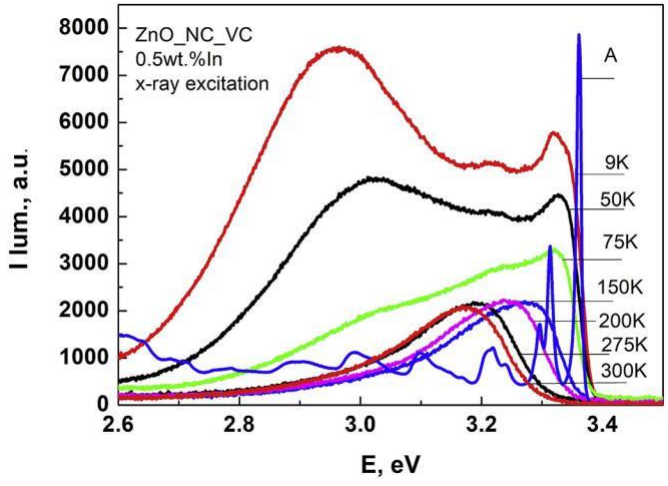

Fig. 3. Temperature dependence of radioluminescence of ZnO:In (0.5 wt%In); A –radioluminescence spectrum of undoped ZnO NC at 9K.

at 300K its contribution is insignificant. In addition, wide band in re-gion 3.0–3.3 eV was detected at 300K and it is interpreted as 1LO_FEx luminescence. Thus, this peak exhibits a scintillation property at 300K. The defect luminescence (450–650 nm) suppressed in samples even with low indium concentration.

Decay times of photoluminescence at 300K were measured with Streak-scope under 266 nm photo excitation. The electrons and holes are produced under 266 nm (4.7eV) excitation which is greater than the band gap, thus the recombination processes and luminescence can be similar to those under x-ray excitation. The decay kinetics were mea-sured at 3.23 eV. Fig. 4a,b shows the fast photoluminescence of un-doped and indium doped ZnO nanopowers. It is observed that the spectra and decay times differ in the undoped and indium doped samples. As one can see the significant broadening of spectra was de-tected in doped samples. The origin of spectra broadening could be due to the exciton interaction with defects incorporated in doped material.

The decay kinetics of photoluminescence (Fig. 5a) were analysed using model only for the falling part of the kinetics. Kinetics were normalized before the analysis. The kinetics can be well approximated by two exponents for all concentrations: the fast component is present

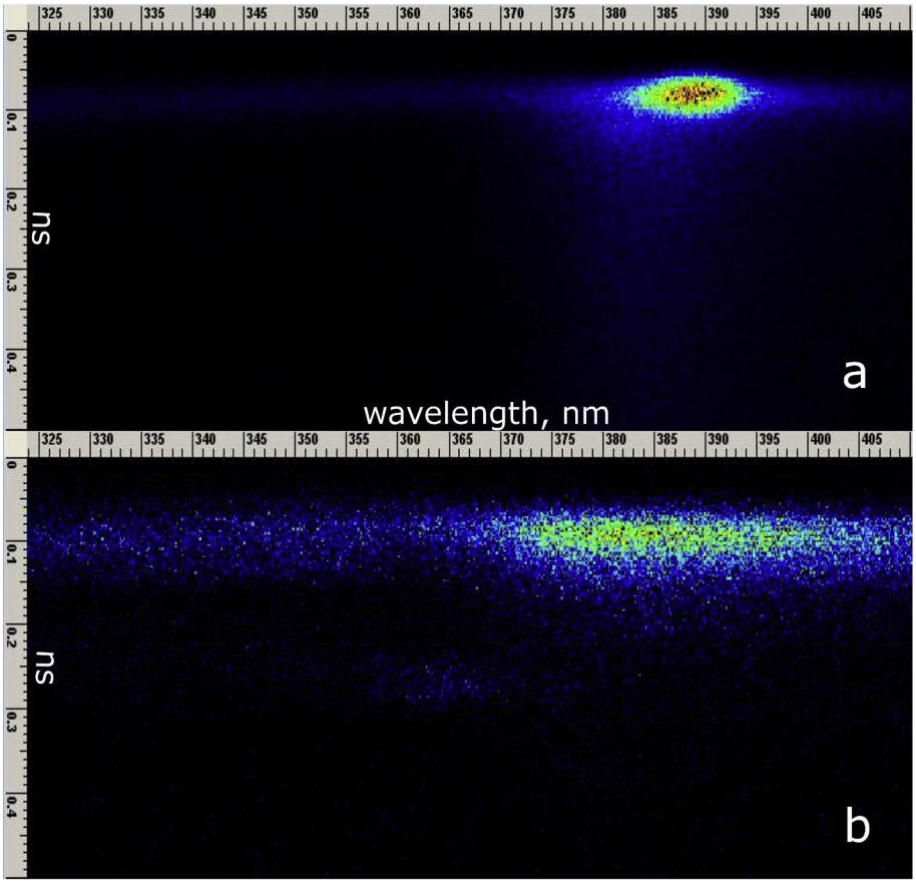

Fig. 4. Streak-camera images of undoped (a) and In-doped ZnO (b) NC (RT).

for all concentrations and is approximately the same; however, the decay time of slow component depends on indium concentration in powder.

Fig. 5b shows the decrease of ~3.24 eV luminescence decay time constant depending on the indium concentration. With increasing in-dium concentration, the decay time decreases. The result shows that changing the indium concentration can change the decay time of fast luminescence. The decrease in the decay time is accompanied by weaker overall luminescence intensity.

5. Summary

The ZnO and ZnO:In nanopowders were successfully synthesized by a SPVD method. Low temperature fast near-edge radioluminescence was measured in all ZnO samples. The results of indium doped nano-powders are compared with ZnO single crystal and undoped ZnO na-nopowders. It was observed that during the synthesis of doped nano-powders the morphology of powders varies and also depends on indium concentration. The excitonic luminescence of ZnO:In is fast: decay time is in sub-nanosecond time region. Decay time in doped nanopowders is less than that of undoped ZnO nanopowders. Two components of the decay were detected with fast component being approximately constant for any indium concentration and slow component varying with the amount of implemented indium atoms in the structure. The defect lu-minescence intensity is significantly suppressed in indium doped sam-ples and the luminescence decay time decreases with increasing indium concentration.

Acknowledgments

The financial support of research European Union ERA.NET RUS_ST20170-51. This work was partly supported by Russian Foundation for Basic Research, Russia, project No.18-52-76002. The sample preparation was carried out as part of SFERA II project - Transnational Access activities (European Union 7th Framework Programme Grant Agreement N3126430).

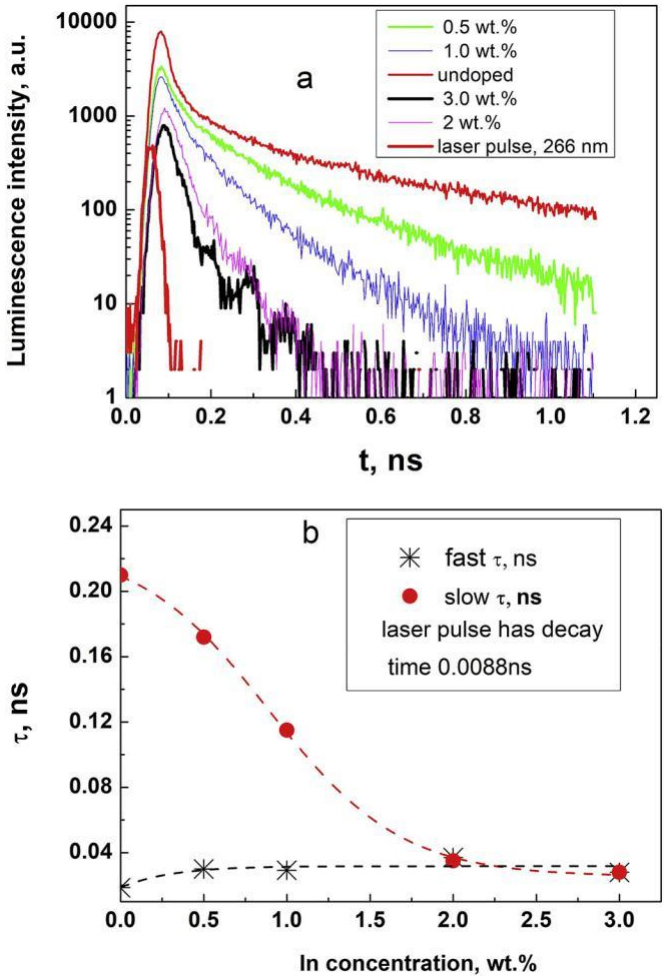

Fig. 5. The decay kinetics of ZnO:In NCs with different In concentration under 266 nm photoexcitation (a) and decay time dependence on In concentration (b).

References

Chernenko, K.A., Gorokhova, E.I., Eron'ko, S.B., Sandulenko, A.V., Venevtsev, I.D., Wieczorek, H., Rodnyi, P.A., 2018. Structural, optical and luminescent properties of ZnO:Ga and ZnO:in ceramics. IEEE Trans. Nucl. Sci. 9499. https://doi.org/10.1109/ TNS.2018.2810331.

Gorokhova, E.I., Eron'ko, S.B., Kul'kov, A.M., Oreshchenko, E.A., Simonova, K.L., Chernenko, K.A., Venevtsev, I.D., Rodnyi, P.A., Lott, K.P., Wieczorek, H., 2015. Development and study of ZnO: in optical scintillation ceramic. J. Opt. Technol. (A Transl. Opt. Zhurnal) 82, 837–842. https://doi.org/10.1364/JOT.82.000837.

Hoel, C.A., Mason, T.O., Gaillard, J.F., Poeppelmeier, K.R., 2010. Transparent conducting oxides in the ZnO-In2O3-SnO2 system. Chem. Mater. 22, 3569–3579. https://doi. org/10.1021/cm1004592.

Kano, M., Wakamiya, A., Sakai, K., Yamanoi, K., Cadatal-Raduban, M., Nakazato, T., Shimizu, T., Sarukura, N., Ehrentraut, D., Fukuda, T., 2011. Response-time-improved ZnO scintillator by impurity doping. J. Cryst. Growth 318, 788–790. https://doi.org/ 10.1016/j.jcrysgro.2010.10.192.

Meyer, B.K., Alves, H., Hofmann, D.M., Kriegseis, W., Forster, D., Bertram, F., Christen, J., Hoffmann, A., Straßburg, M., Dworzak, M., Haboeck, U., Rodina, A.V., 2004. Bound exciton and donor-acceptor pair recombinations in ZnO. Phys. Status Solidi Basic Res. 241, 231–260. https://doi.org/10.1002/pssb.200301962.

Rodnyi, P.A., Gorokhova, E.I., Chernenko, K.A., Khoduk, I.V., 2012. Scintillating ceramics based on zinc oxide. IOP Conf. Ser. Mater. Sci. Eng. 38, 1–8. https://doi.org/10. 1088/1757-899X/38/1/012002.

Smits, K., Grigorjeva, L., Millers, D., Kundzins, K., Ignatans, R., Grabis, J., Monty, C., 2014. Luminescence properties of zirconia nanocrystals prepared by solar physical vapor deposition. Opt. Mater. (Amst). 37, 251–256. https://doi.org/10.1016/j. optmat.2014.06.003.

Wienke, J., Booi, A.S., 2008. ZnO:In deposition by spray pyrolysis - influence of growth conditions on the electrical and optical properties. Thin Solid Films 516, 4508–4512.

Wilkinson, J., Ucer, K.B., Williams, R.T., 2004. Picosecond excitonic luminescence in ZnO and other wide-gap semiconductors. Radiat. Meas. 38, 501–505. https://doi.org/10. 1016/j.radmeas.2004.01.022.

Xiong, G., Ucer, K.B., Williams, R.T., Lee, J., Bhattacharyya, D., Metson, J., Evans, P., 2005. Donor-acceptor pair luminescence of nitrogen-implanted ZnO single crystal. J. Appl. Phys. 97. https://doi.org/10.1063/1.1854208.

Institute of Solid State Physics, University of Latvia as the Center of Excellence has received funding from the European Union's Horizon 2020 Framework Programme H2020-WIDESPREAD-01-2016-2017-TeamingPhase2 under grant agreement No. 739508, project CAMART²